Predictive Control at Fixed Switching Frequency for a Dual Three-Phase Induction Machine with Kalman Filter-Based Rotor Estimator

Magno Ayala, Osvaldo Gonzalez, Jorge Rodas, *Member, IEEE,*, Raul Gregor, *Member, IEEE,* and Marco Rivera, *Member, IEEE*

***Abstract*—Classic finite-set model predictive control techniques are distinguished by a variable switching frequency which causes noise, large voltage and current ripple. This paper presents an enhanced predictive current control technique with fixed switching frequency applied to the six-phase drives and a Kalman Filter estimator. Simulation results are provided to show the efficiency of the current control algorithm using the mean square error and total harmonic distortion as a figures of merit, thus concluding that the system can work properly with this enhanced technique.**

***Index Terms*—Multiphase machine, predictive current control, fixed switching frequency, Kalman filter.**

I. Introduction

RECENTLY, the interest in multiphase machines has risen due to intrinsic features such as lower torque ripple, power splitting or better fault tolerance than three-phase machines. Current research works and developments support the prospect of future more widespread applications of multiphase machines [1]. In industrial applications, any multiphase machine would be operated under variable-speed conditions, meaning that a multiphase power electronic converter is required [2].

Due to technological advances and the emergence of faster microcontrollers with capability of more powerful calculations, the implementation of nonlinear and complex control techniques, such as sliding mode control, fuzzy control, adaptive control, and predictive control, has become more promising [3]. In the last years, predictive control has gained greater interest because of some distinct properties such as intrinsic decoupling characteristics, fast dynamic response and high bandwidth [4]. Model predictive control (MPC) is very intuitive and easy to implement, however, this control strategy provides a variable switching frequency. A main obstacle of the MPC methods is that the control can only select from a finite number of valid switching states because of the absence of a modulator. This generates distortion as well as large current and voltage ripples. On the other hand, the variable switching frequency produces a spread spectrum, decreasing the performance of the system in terms of power quality [5].Finite State (FS)-MPC uses a suitable modulation scheme in the cost function minimization of the predictive algorithm for a selected number of switching states to generate the duty cycles for two active vectors and two zero vectors which are applied to the converter using a given switching pattern in order to obtain an efficient dynamic of the system [6].

This paper proposes a predictive-fixed switching frequency technique for current control of a dual three-phase induction machine (DTPIM) and a reduced order estimator based on a Kalman filter (KF) to estimate the rotor current. The efficiency of the proposed algorithm is analyzed by using the mean square error (MSE) and the total harmonic distortion (THD) as a figures of merit. The proposed technique is tested for different current reference frequencies.

This paper is organized as follows. Section II describes the DTPIM drive and presents the mathematical model of the DTPIM. Section III details the predictive model with the current control with rotor current estimator based on KF and presents the proposed FS-MPC method for the DTPIM. Simulation results are provided in Section IV, showing the efficiency obtained by the current tracking. The conclusions are summarized in the last section.

II. The Dual Three-Phase Induction Machine Drive

The system under study consists of a DTPIM fed by a six-phase voltage source inverter (VSI) and a dc-link. A detailed scheme of the drive is provided in Fig. 1.

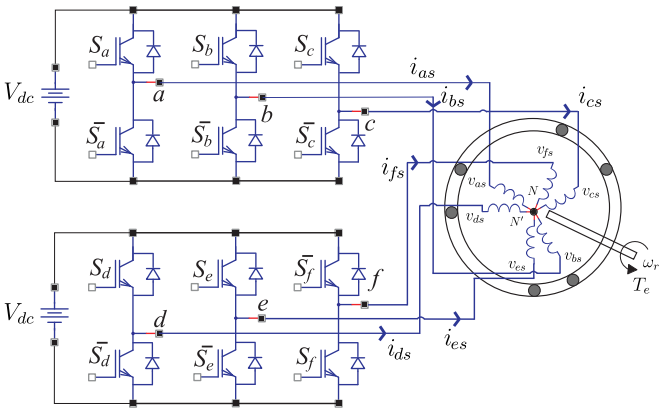

Fig. 1. A general scheme of a dual three-phase induction machine.

M. Ayala, O. Gonzalez, J. Rodas and R. Gregor are with the Laboratory of Power and Control Systems, Faculty of Engineering, Universidad Nacional de Asunción, Paraguay e-mail: mayala, ogonzalez, jrodas & rgregor @ing.una.py (see http://www.dspyc.com.py/).

M. Rivera is with the Department of Electrical Engineering, Faculty of Engineering, Universidad de Talca, Curicó, PB, 3341717 Chile e-mail: marcoriv@utalca.cl (see https://marcorivera.cl/).

9781509011476/16/$31.00

This DTPIM is a continuous system which can be described by a set of differential equations. The model of the system can be simplified by means of the vector space decomposition (VSD). By applying this technique, the original six-dimensional space of the machine is transformed into three two-dimensional orthogonal subspaces in the stationary reference frame $(\alpha-\beta)$, $(x-y)$ and (z_1-z_2). This transformation is obtained by means of 6 x 6 transformation matrix:

$$\mathbf{T}=\frac{1}{3}\begin{bmatrix} 1 & \frac{\sqrt{3}}{2} & -\frac{1}{2} & -\frac{\sqrt{3}}{2} & -\frac{1}{2} & 0 \\ 0 & \frac{1}{2} & \frac{\sqrt{3}}{2} & \frac{1}{2} & -\frac{\sqrt{3}}{2} & -1 \\ 1 & -\frac{\sqrt{3}}{2} & -\frac{1}{2} & \frac{\sqrt{3}}{2} & -\frac{1}{2} & 0 \\ 0 & \frac{1}{2} & -\frac{\sqrt{3}}{2} & \frac{1}{2} & \frac{\sqrt{3}}{2} & -1 \\ 1 & 0 & 1 & 0 & 1 & 0 \\ 0 & 1 & 0 & 1 & 0 & 1 \end{bmatrix}\begin{matrix}\alpha\\ \beta\\ x\\ y\\ z_1\\ z_2\end{matrix} \tag{1}$$

where an amplitude invariant criterion was used.

The VSI has a discrete nature, it has a total number of $2^6 = 64$ different switching states defined by six switching functions corresponding to the six inverter legs $[S_a, S_b, S_c, S_d, S_e, S_f]$, where $\mathbf{S}_i \in \{0, 1\}$. The different switching states and the voltage of the dc-link (V_{dc}) define the phase voltages which can in turn be mapped to the $(\alpha-\beta)-(x-y)$ space according to the VSD approach [7].

As it is shown in Fig. 2 the 64 possibilities lead to only 49 different vectors in the $(\alpha-\beta)-(x-y)$ subspace.

The machine can be modeled by using an state-space representation, based on the VSD approach and the dynamic reference transformation. This model is given by:

$$\begin{aligned}\frac{d}{dt}(\mathbf{X}_{\alpha\beta xy}) &= \mathbf{A}\mathbf{X}_{\alpha\beta xy}+\mathbf{B}\mathbf{U}_{\alpha\beta xy}\\ \mathbf{Y}_{\alpha\beta xy} &= \mathbf{C}\mathbf{X}_{\alpha\beta\mathbf{xy}}\end{aligned} \tag{2}$$

where:

$$\begin{aligned}\mathbf{U}_{\alpha\beta xy} &= \begin{bmatrix} u_{\alpha s} & u_{\beta s} & u_{xs} & u_{ys} & 0 & 0\end{bmatrix}^T\\ \mathbf{X}_{\alpha\beta xy} &= \begin{bmatrix} i_{\alpha s} & i_{\beta s} & i_{xs} & i_{ys} & i_{\alpha r} & i_{\beta r}\end{bmatrix}^T\\ \mathbf{Y}_{\alpha\beta xy} &= \begin{bmatrix} i_{\alpha s} & i_{\beta s} & i_{xs} & i_{ys} & 0 & 0\end{bmatrix}^T\end{aligned} \tag{3}$$

being $\mathbf{U}_{\alpha\beta xy}$ the input vector of the system, $\mathbf{X}_{\alpha\beta xy}$ the state vector, $\mathbf{Y}_{\alpha\beta xy}$ indicates the output vector, the superscript $(^T)$ indicates the transposed matrix and $\mathbf{A}$, $\mathbf{B}$ and $\mathbf{C}$ are matrices that define the dynamics of the electrical drive.

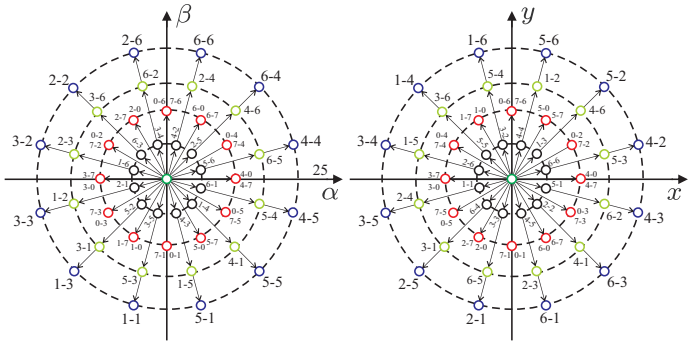

Fig. 2. Voltage space vectors and switching states in the $(\alpha-\beta)$ and $(x-y)$ subspaces for a dual three-phase VSI.

The mechanical part of the electrical drive is given by the following equations:

$$T_e = 3P\left(\psi_{\alpha s} i_{\beta s} - \psi_{\beta s} i_{\alpha s}\right) \tag{4}$$

$$J_i \frac{d}{dt}\omega_r + B_i\omega_r = P\left(T_e - T_L\right) \tag{5}$$

where T_L denotes the load torque, T_e is the generated torque, J_i the inertia coefficient, P the number of pairs of poles, $\psi_{\alpha s}$ and $\psi_{\beta s}$ the stator flux, B_i the friction coefficient and ω_r is the rotor angular speed.

III. Proposed Predictive Control Method

Assuming the mathematical model expressed by (2) and using the state variables defined by the vector $\mathbf{X}_{\alpha\beta xy}$, we can define the following set of equations:

$$\begin{aligned}\frac{d}{dt}(x_1) &= -R_s c_2 x_1 + c_4\left(L_m\omega_r x_2 + R_r x_5 + L_r\omega_r x_6\right)\\ &\quad + c_2 u_1\\ \frac{d}{dt}(x_2) &= -R_s c_2 x_2 + c_4\left(-L_m\omega_r x_1 - L_r\omega_r x_5 + R_r x_6\right)\\ &\quad + c_2 u_2\\ \frac{d}{dt}(x_3) &= -R_s c_3 x_3 + c_3 u_3\\ \frac{d}{dt}(x_4) &= -R_s c_3 x_4 + c_3 u_4\\ \frac{d}{dt}(x_5) &= -R_s c_4 x_1 + c_5\left(-L_m\omega_r x_2 - R_r x_5 - L_r\omega_r x_6\right)\\ &\quad - c_4 u_1\\ \frac{d}{dt}(x_6) &= -R_s c_4 x_2 + c_5\left(L_m\omega_r x_1 + L_r\omega_r x_5 - R_r x_6\right)\\ &\quad - c_4 u_2\end{aligned} \tag{6}$$

where R_s, $L_s = L_{ls} + L_m$, R_r, $L_r = L_{lr} + L_m$ and L_m are the electrical parameters of the machine. The coefficients c_i for $i = 1, \ldots, 5$, are defined as $c_1 = L_s L_r - L_m^2$, $c_2 = \frac{L_r}{c_1}$, $c_3 = \frac{1}{L_{ls}}$, $c_4 = \frac{L_m}{c_1}$ and $c_5 = \frac{L_s}{c_1}$, while the input vector corresponds to the voltages applied to the stator $u_1 = v_{\alpha s}$, $u_2 = v_{\beta s}$, $u_3 = v_{xs}$, $u_4 = v_{ys}$ and the state vector corresponds to the DPTIM currents $x_1 = i_{\alpha s}$, $x_2 = i_{\beta s}$, $x_3 = i_{xs}$, $x_4 = i_{ys}$, $x_5 = i_{\alpha r}$ and $x_6 = i_{\beta r}$.

Stator voltages are related to the input control signals through the inverter model. In this case, the simplest model has been considered for the sake of speeding up the optimization process. Then if the gating signals are arranged in the vector $\mathbf{S} = [S_a, S_b, S_c, S_d, S_e, S_f]$, where the stator voltages can be obtained from:

$$\mathbf{M}=\frac{1}{3}\begin{bmatrix} 2 & 0 & -1 & 0 & -1 & 0 \\ 0 & 2 & 0 & -1 & 0 & -1 \\ -1 & 0 & 2 & 0 & -1 & 0 \\ 0 & -1 & 0 & 2 & 0 & -1 \\ -1 & 0 & -1 & 0 & 2 & 0 \\ 0 & -1 & 0 & -1 & 0 & 2 \end{bmatrix}\cdot\mathbf{S}^T \tag{7}$$

An ideal inverter converts gating signals into stator voltages that can be projected to $(\alpha-\beta)$ and $(x-y)$ subspaces and gathered in a row vector $\mathbf{U}_{\alpha\beta xys}$ computed as:

$$\mathbf{U}_{\alpha\beta xys} = [u_{\alpha s}\, u_{\beta s}\, u_{xs}\, u_{ys}\, 0\, 0]^T = V_{dc}\cdot\mathbf{T}\cdot\mathbf{M} \tag{8}$$

By combining (6)-(8) a nonlinear set of equations arises that can be written in state-space form:

$$\begin{aligned}\frac{d}{dt}(\mathbf{X}_{(t)}) &= f\left[\mathbf{X}_{(t)},\, \mathbf{U}_{(t)}\right]\\ \mathbf{Y}_{(t)} &= \mathbf{C}\mathbf{X}_{(t)}\end{aligned} \tag{9}$$

with state vector $\mathbf{X}_{(t)} = [x_1,\, x_2,\, x_3,\, x_4, x_5,\, x_6]^T$, input vector $\mathbf{U}_{(t)} = [u_1,\, u_2, u_3,\, u_4]$, and $\mathbf{Y}_{(t)} = [x_1,\, x_2, x_3,\, x_4]^T$ as the output vector. The components of the vectorial function f and the matrix $\mathbf{C}$ are obtained in a straightforward manner from (6) and the definitions of state and output vector. Model (9) must be discretized in order to be of used for the predictive controller. A forward-Euler method is used to keep a low computational cost. Due to this fact, the resulting equations will have the required digital control form, with predicted variables depending just on past values and not on present values of the variables. Thus, a prediction of the future next-sample state $\hat{\mathbf{X}}_{[k+1|k]}$ is expressed as:

$$\hat{\mathbf{X}}_{[k+1|k]} = \mathbf{X}_{[k]} + T_m f\left(\mathbf{X}_{[k]},\, \mathbf{U}_{[k]},\, \omega_{r[k]}\right) \tag{10}$$

where k is the current sample and T_m the sampling time.

A. Reduced order estimators

In the state-space description (9) only stator currents, voltages and mechanical speed are measured. Stator voltages are easily predicted from the gating commands issued to the VSI, rotor current, however, cannot be directly measured. This difficulty can be overcome by means of estimating the rotor current using the concept of reduced order estimators.

The reduced order estimators provide an estimate for only the unmeasured part of the state vector, then, the evolution of states can be written as:

$$\underbrace{\begin{bmatrix}\hat{\mathbf{X}}_{a[k+1|k]}\\ \hat{\mathbf{X}}_{b[k+1|k]}\\ \hat{\mathbf{X}}_{c[k+1|k]}\end{bmatrix}}_{[\hat{\mathbf{X}}_{[k+1|k]}]} = \underbrace{\begin{bmatrix}\overline{\mathbf{A}}_{11} & \overline{\mathbf{A}}_{12} & \overline{\mathbf{A}}_{13}\\ \overline{\mathbf{A}}_{21} & \overline{\mathbf{A}}_{22} & \overline{\mathbf{A}}_{23}\\ \overline{\mathbf{A}}_{31} & \overline{\mathbf{A}}_{32} & \overline{\mathbf{A}}_{33}\end{bmatrix}}_{[\mathbf{A}]}\underbrace{\begin{bmatrix}\mathbf{X}_{a[k]}\\ \mathbf{X}_{b[k]}\\ \mathbf{X}_{c[k]}\end{bmatrix}}_{[\mathbf{X}_{[k]}]} + \underbrace{\begin{bmatrix}\overline{\mathbf{B}}_1\\ \overline{\mathbf{B}}_2\\ \overline{\mathbf{B}}_3\end{bmatrix}^T}_{[\mathbf{B}]}\underbrace{\begin{bmatrix}\mathbf{U}_{\alpha\beta s}\\ \mathbf{U}_{xys}\\ \mathbf{U}_{\alpha\beta s}\end{bmatrix}}_{[\mathbf{U}_k]} \tag{11}$$

$$\mathbf{Y}_{[k]} = \underbrace{\begin{bmatrix}\overline{\mathbf{I}} & \overline{\mathbf{I}} & \overline{\mathbf{0}}\end{bmatrix}}_{[\mathbf{C}]}\underbrace{\begin{bmatrix}\mathbf{X}_{a[k]}\\ \mathbf{X}_{b[k]}\\ \mathbf{X}_{c[k]}\end{bmatrix}}_{[\mathbf{X}_{[k]}]} \tag{12}$$

where $\mathbf{X}_a = [\, i_{\alpha s}\quad i_{\beta s}\,]^T$, $\mathbf{X}_b = [\, i_{xs}\quad i_{ys}\,]^T$, $\mathbf{X}_c = [\, i_{\alpha r}\quad i_{\beta r}\,]^T$, $\mathbf{U}_{\alpha\beta s} = [\, U_{\alpha s}\quad U_{\beta s}\,]^T$, $\mathbf{U}_{xys} = [\, U_{xs}\quad U_{ys}\,]^T$.

B. Rotor state estimation based on Kalman filters

The rotor currents's estimation is a complex problem that has been recently solved using different methods [8], [9], being KF-based estimator the best choice, which considers uncorrelated process and zero-mean Gaussian measurement noises, thus the systems equations can be written as:

$$\hat{\mathbf{X}}_{[k+1|k]} = \mathbf{A}\mathbf{X}_{[k]} + \mathbf{B}\mathbf{U}_{[k]} + \mathbf{H}\varpi_{[k]} \tag{13}$$

$$\mathbf{Y}_{[k+1|k]} = \mathbf{C}\mathbf{X}_{[k+1]} + \nu_{[k+1]} \tag{14}$$

where $\varpi_{[k]}$ is the process noise, $\mathbf{H}$ is the noise weight matrix and $\nu_{[k+1]}$ is the measurement noise.

The dynamics of the KF can be written as shown in [8] and has not been included for the sake of conciseness.

$$\begin{aligned}\hat{\mathbf{X}}_{c[k+1|k]} = (\mathbf{A}_{33} - \mathbf{K}_{[k]}\mathbf{A}_{13})\hat{\mathbf{X}}_{c[k]} + \mathbf{K}_{[k]}\mathbf{Y}_{[k+1]} +\\ (\mathbf{A}_{31} - \mathbf{K}_{[k]}\mathbf{A}_{11})\mathbf{Y}_{[k]} + (\mathbf{B}_3 - \mathbf{K}_{[k]}\mathbf{B}_1)\mathbf{U}_{\alpha\beta s[k]}\end{aligned} \tag{15}$$

where $\mathbf{K}$ is the KF gain matrix which is calculated from the covariance of the noises at each sampling time.

C. Cost function

The cost function should include all terms to be optimized. In current control the most important figure is the tracking error in the predicted stator currents for the next sample. To minimize its magnitude for each sample k it suffices to use a simple expression such as:

$$\begin{aligned}J_{[k+2|k]} =& \hat{e}_{i\alpha s[k+2]} + \hat{e}_{i\beta s[k+2]} + \lambda_{xy}\left(\hat{e}_{ixs[k+2]} + \hat{e}_{iys[k+2]}\right)\\ \hat{e}_{i\alpha s[k+2]} =& \parallel i^*_{\alpha s[k+2]} - \hat{i}_{\alpha s[k+2]} \parallel^2\\ \hat{e}_{i\beta s[k+2]} =& \parallel i^*_{\beta s[k+2]} - \hat{i}_{\beta s[k+2]} \parallel^2\\ \hat{e}_{ixs[k+2]} =& \parallel i^*_{xs[k+2]} - \hat{i}_{xs[k+2]} \parallel^2\\ \hat{e}_{iys[k+2]} =& \parallel i^*_{ys[k+2]} - \hat{i}_{ys[k+2]} \parallel^2\end{aligned} \tag{16}$$

where $\parallel\ .\ \parallel$ denotes vector magnitude, λ_{xy} is a tuning parameter which gives more redundance to $(\alpha-\beta)$ subspace, $i^*_{s[k+2]}$ is a vector containing the reference for the stator currents and $\hat{i}_{s[k+2]}$ is a vector containing the predictions based on the next state (including the delay compensation).

D. Proposed predictive control technique

It is feasible to determine each available vector for the VSI in the $(\alpha-\beta)$ plane, which defines 64 sectors (48 different), which are given by two adjacent vectors, as shown in Fig. 3.

The proposed technique evaluates the prediction of the two active vectors that conform each sector at every sampling time and evaluates the cost function separately for each prediction [6]. The cost function, defined by (16), is evaluated for each case and is the same as the one considered for the variable frequency predictive method. For example, for sector I, the first prediction and cost function J_1 is evaluated for vector V_{4-4} and the second prediction and cost function J_2 is evaluated for vector V_{6-4}. Each prediction is evaluated based on (6) and the only change is in respect to the calculation of

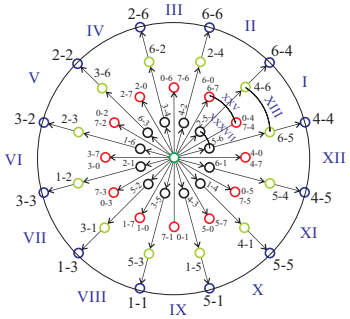

Fig. 3. Available sectors for the VSI.

the input vector $\mathbf{U}$. The duty cycles, for the two active vectors, are calculated by solving the following equations:

$$d_0 = \frac{\delta}{J_0} \qquad d_1 = \frac{\delta}{J_1} \qquad d_2 = \frac{\delta}{J_2} \tag{17}$$

$$d_0 + d_1 + d_2 = T_m \tag{18}$$

where d_0 correspond to the duty cycle of a zero vector which is evaluated only one time. By solving (17)-(18) is possible to obtain the expression for δ and the expressions for the duty cycles for each vector are given as:

$$d_0 = \frac{T_m J_1 J_2}{J_0 J_1 + J_1 J_2 + J_0 J_2} \tag{19}$$

$$d_1 = \frac{T_m J_0 J_2}{J_0 J_1 + J_1 J_2 + J_0 J_2} \tag{20}$$

$$d_2 = \frac{T_m J_0 J_1}{J_0 J_1 + J_1 J_2 + J_0 J_2} \tag{21}$$

Considering these expressions, the new cost function, which is evaluated at every sampling time, is defined as:

$$G_{[k+2|k]} = d_1 J_1 + d_2 J_2 \tag{22}$$

The two vectors that minimize (22) are selected and applied to the VSI at the next sampling time. Thus, the proposed control technique selects the control actions by solving an optimization problem for each sampling period. A model of the DTPIM, is used to predict its output. This prediction is carried out for each possible sector of the six-phase inverter to determine which one minimizes a defined cost function represented by (22). Therefore, the model of the real system, also called predictive model, must be used considering all possible voltage sectors in the six-phase inverter. Finally, after obtaining the duty cycles and selecting the optimal two vectors to be applied, a switching pattern procedure, shown in Fig. 4, is adopted with the goal of applying the two active vectors $(v_1 - v_2)$ and two zero vectors (v_0) [10], considering:

$$\begin{aligned} T_0 &= d_0 \cdot step \\ T_1 &= d_1 \cdot step \\ T_2 &= d_2 \cdot step \end{aligned} \tag{23}$$

where $step$ is the number of steps in a sample time.

A detailed block diagram of the predictive current control (PCC) technique for the DTPIM drive is provided in Fig. 5.

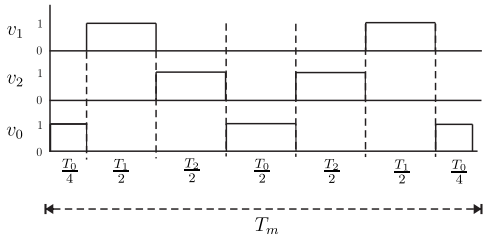

Fig. 4. Switching pattern for the optimal vectors.

IV. Simulation Results

A MATLAB/Simulink simulation environment has been designed for the VSI-fed DTPIM. Simulation tests have been performed to show the efficiency of the PCC technique. Numerical integration using first order Euler's method has been applied to compute the evolution of the state variables in the time domain. Table I shows the parameters for the DTPIM.

TABLE I
Parameters of the DTPIM

PARAMETER	SYMBOL	VALUE	UNIT
Stator resistance	R_s	0.62	Ω
Rotor resistance	R_r	0.63	Ω
Stator inductance	L_s	206.2	mH
Rotor inductance	L_r	203.3	mH
Magnetizing inductance	L_m	199.8	mH
System inertia	J_i	0.27	kg.m^2
Pairs of poles	P	3	–
Friction coefficient	B_i	0.012	kg.m^2/s

The cost function defined in (16) with λ_{xy} = 0.001, was used to evaluated the dynamic performance of the PCC and the estimated noise covariances for $\varpi_{[k]}$ and $\nu_{[k+1]}$ were 0.0022. The efficiency of the PCC has been evaluated, under load condition of 2 N·m. In all cases, are considered a sampling frequency of 50 kHz and the number of steps of 20, giving a total of 1000 ksps. Fig. 6 shows the simulation results for a current reference with different frequencies, with a fixed reference current amplitude of 2 A. It is shown the switching in the VSI, showing the pattern of the modulation technique and the THD of the measured stator current in different

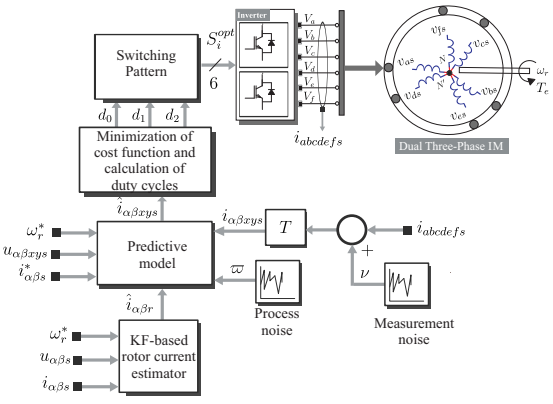

Fig. 5. Proposed predictive current control technique for the DTPIM.

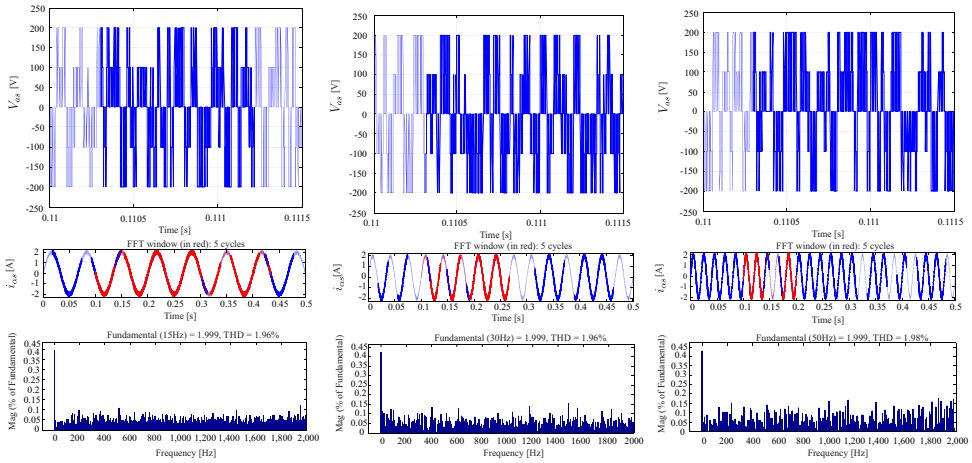

(a) (b) (c)

Fig. 6. THD analysis of the measured current $i_{\alpha s}$. Simulation results for current frequency of: (a) 15 Hz; (b) 30 Hz; (c) 50 Hz.

frequencies. Fig. 7 shows the current response with reference changes. Under these test conditions, MSE and THD in the current tracking (in steady state) are indicated on Table II.

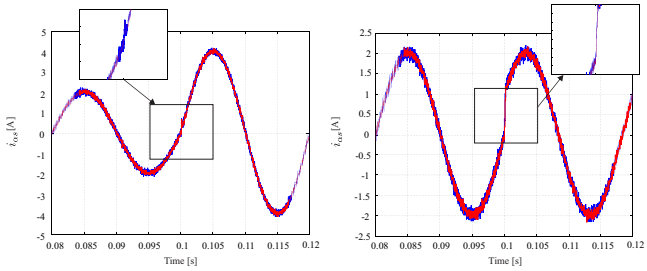

(a) (b)

Fig. 7. Predictive-fixed switching frequency response with modified reference at 0.1 s, (a) Step change from 2 A to 4 A; (b) Phase 30°.

TABLE II
PERFORMANCE ANALYSIS

fe (Hz)	MSE$_\alpha$	MSE$_\beta$	THD$_\alpha$ (%)	THD$_\beta$ (%)
5	0.082	0.09	1.97	2.17
10	0.082	0.091	2.01	2.19
15	0.083	0.094	1.96	2.19
20	0.081	0.091	2.00	2.16
25	0.082	0.091	1.99	2.18
30	0.082	0.092	1.96	2.18
35	0.081	0.09	1.94	2.15
40	0.081	0.09	2.04	2.20
45	0.082	0.091	1.96	2.15
50	0.082	0.092	1.98	2.16

V. CONCLUSION

In this paper, a predictive-fixed switching frequency technique for current control in a DTPIM is proposed. The MPC is designed through a state-space representation, where the rotor and stator current are the state variables. The theoretical development of the predictive-fixed switching controller has been validated through simulation results, which demonstrate that this is a viable alternative to obtain a great performance in both steady and transient conditions with a good current tracking, a reduced ripple and a symmetric use of the switches.

ACKNOWLEDGMENT

The authors would like to thank to the Paraguayan Government for the economical support provided by means of a CONACYT grant project 14-INV-101 and also to the financial support of FONDECYT into Research Regular 1160690.

REFERENCES

[1] F. Barrero and M. J. Duran, "Recent advances in the design, modeling, and control of multiphase machines part I," *IEEE Trans. Ind. Electron.*, vol. 63, no. 1, pp. 449–458, 2016.

[2] E. Levi, "Advances in converter control and innovative exploitation of additional degrees of freedom for multiphase machines," *IEEE Trans. Ind. Electron.*, vol. 63, no. 1, pp. 433–448, 2016.

[3] J. Rodriguez, M. P. Kazmierkowski, J. R. Espinoza, P. Zanchetta, H. Abu-Rub, H. A. Young, and C. A. Rojas, "State of the art of finite control set model predictive control in power electronics," *IEEE Trans. Ind. Informatics*, vol. 9, no. 2, pp. 1003–1016, 2013.

[4] M. Rivera, M. Perez, V. Yaramasu, B. Wu, L. Tarisciotti, P. Zanchetta, and P. Wheeler, "Modulated model predictive control (m 2 pc) with fixed switching frequency for an npc converter," in *Proc. POWERENG*, 2015, pp. 623–628.

[5] M. Vijayagopal, P. Zanchetta, L. Empringham, L. De Lillo, L. Tarisciotti, and P. Wheeler, "Modulated model predictive current control for direct matrix converter with fixed switching frequency," in *Proc. EPE*, 2015, pp. 1–10.

[6] M. Rivera, F. Morales, C. Baier, J. Munoz, L. Tarisciotti, P. Zanchetta, and P. Wheeler, "A modulated model predictive control scheme for a two-level voltage source inverter," in *Proc. ICIT*, 2015, pp. 2224–2229.

[7] R. Gregor, J. Rodas, D. Gregor, and F. Barrero, *Reduced-order observer analysis in MBPC techniques applied to the six-phase induction motor drives*. INTECH Open Science, 2015.

[8] J. Rodas, F. Barrero, M. R. Arahal, C. Martin, and R. Gregor, "On-line estimation of rotor variables in predictive current controllers: A case study using five-phase induction machines," *IEEE Trans. Ind. Electron.*, vol. PP, no. 99, pp. 1–1, 2016.

[9] C. Martin, M. Arahal, F. Barrero, and M. Duran, "Five-phase induction motor rotor current observer for finite control set model predictive control of stator current," *IEEE Trans. Ind. Electron.*, vol. PP, no. 99, pp. 1–1, 2016.

[10] S. Vazquez, A. Marquez, R. Aguilera, D. Quevedo, J. I. Leon, and L. G. Franquelo, "Predictive optimal switching sequence direct power control for grid-connected power converters," *IEEE Trans. Ind. Electron.*, vol. 62, no. 4, pp. 2010–2020, 2015.

Magno Ayala received the B.Eng. degree in electronic engineering from the Universidad Nacional de Asunción (UNA), Paraguay, in 2014. He joined the Laboratory of Power and Control System at the UNA, in 2015, working as a Research Assistant, and since 2015, he's working toward the MSc. degree in Power Electronics. He is currently a Associated Researcher in the Laboratory of Power and Control System, Universidad Nacional de Asunción, Paraguay. Mr. Ayala is a recipient of the training program for university lecturers from the CONACYT of Paraguay for his MSc. studies.

Osvaldo Gonzalez was born in Paraguay in 1987. B.Eng. degree in electronic engineering from the Universidad Nacional de Asunción (UNA), in 2014, where he is currently working toward the MSc. degree in Power Electronics. His research interests include the area of control of multiphase motors. Mr. Gonzalez is a recipient of the training program for university lecturers from the CONACYT of Paraguay for his MSc. studies.

Jorge Rodas (S'08–M'12) was born in Asunción, Paraguay in 1984. He received his B.Eng. degree in Electronic Engineering from the Universidad Nacional de Asunción (UNA), Paraguay, in 2009. He received his M.Sc. degrees from the Universidad de Vigo, Spain, in 2012 and from the Universidad de Sevilla, Spain, in 2013, and his joint-university Ph.D. degree between the Universidad Nacional de Asunción and the Universidad de Sevilla in 2016.

In 2011, he joined the Laboratory of Power and Control System at the UNA, where he is currently an Associate Professor. His main research areas are predictive control, multiphase drives, matrix converters and control of power converters for renewable energy applications.

Raúl Gregor was born in Asunción, Paraguay, in 1979. He received the Bachelor Degree in Electronic Engineering from the Catholic University of Asunción, Paraguay, in 2005. He received the M.Sc. and Ph.D. degrees in Electronic, Signal Processing and Communications from the Higher Technical School of Engineering (ETSI), University of Seville, Spain, in 2008 and 2010, respectively. Since March 2010, Prof. Gregor is Head of the Laboratory of Power and Control System (LSPyC) of the Engineering Faculty in the National University of Asuncion, Paraguay.

Prof. Gregor has authored or coauthored about 40 technical papers in the field of power electronics and control systems, six of which have been published in high impact factor journals. He obtained the Best Paper Award from the IEEE TRANSACTIONS ON INDUSTRIAL ELECTRONICS, Industrial Electronics Society, in 2010, and the Best Paper Award from the IET ELECTRIC POWER APPLICATIONS, in 2012. His research interests include; Multiphase Drives, Advanced Control of Power Converters Topologies, Quality of Electrical Power, Renewable Energy, Modelling, Simulation, Optimization and Control of Power Systems, Smart Metering & Smart Grids and Predictive Control.

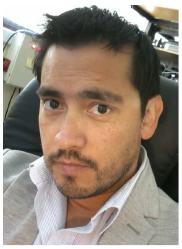

Marco Rivera (S'09-M'11) was born in Talca, Chile, in 1982. He received the B.Sc. degree in electronics engineering and the M.Sc. degree in electrical engineering from the Universidad de Concepción, Concepción, Chile, in 2007 and 2008, respectively, and the Ph.D. degree from the Department of Electronics Engineering, Universidad Técnica Federico Santa María, Valparaíso, Chile, in 2011.

Since 2013 is with the Energy Conversion and Power Electronics Research Group at the Universidad de Talca. He is currently an Associate Professor with the Department of Electrical Engineering at the Universidad de Talca, Curicó, Chile. His main research areas are digital control applied to power electronics, matrix converters, predictive control and control of power converters for renewable energy applications.

Prof. Rivera was recipient of the Best PhD Thesis Award 2012, award given by the Chilean Academy of Science for PhD thesis developed in 2011 by national and foreign students in any Exact or Nature Sciences Program in Chile. In August 2015, Prof. Rivera was awarded with the Outstanding Engineer 2015 Award of the Electrical-Electronics Industry Association and the IEEE-Chile Section and also he received the Second Prize Paper Award in the 2015 IEEE Journal of Emerging and Selected Topics in Power Electronics.